NMR and Structural Model of Dynorphin A (1−17) Bound to Dodecylphosphocholine Micelles†

Michael R. Tessmer and Deborah A. Kallick*

Department of Medicinal Chemistry, College of Pharmacy, University of Minnesota, 308 Harvard Street SE, Minneapolis, Minnesota 55455

Received June 19, 1996; Revised Manuscript Received November 27, 1996⊗

ABSTRACT: Dynorphin A (1−17) (dynorphin) acts preferentially and with high affinity at the κ-opioid receptor, for which it is the natural, endogenous ligand. Interest in designing new ligands to interact at the κ-opioid receptor is based in part on the desire to circumvent some of the problems associated with μ-opioid ligands such as morphine. The high-resolution structure of dynorphin in an environment which closely resembles its environment *in vivo* could be considered as an important lead for new drugs. The interactions that occur between dynorphin and a model membrane are potentially important, as peptide hormone activity is thought to be mediated by interactions with the cell membrane. Therefore, we have determined the high-resolution structures of dynorphin in a model membrane. Results from our laboratory have shown the existence of an α-helical region in dynorphin from residues Gly^3 through Arg^9 when bound to perdeuterated dodecylphosphocholine (DPC) micelles. In this report we show that dynorphin is bound to DPC micelles and describe a family of dynorphin structures that is α-helical from residues Gly^3 through Pro^{10} and that contains a β-turn from residues Trp^{14} through Gln^{17}. A model of interaction with the micelle is also reported and is discussed in the context of hormone action *in vivo.* The structures were determined with 1D and 2D nuclear magnetic resonance spectroscopy, distance geometry in dihedral angle space, and restrained molecular dynamics simulations.

Opioid peptides continue to be of tremendous interest because of their diversity of function and potential for analgesia. It has now been established that the opioid receptor has at least three types: μ, δ, and κ (Brownstein, 1993). Dynorphin A (1−17) (dynorphin)[1] is a κ-opioid receptor agonist that binds with high affinity and is presumed to be the endogenous ligand (Goldstein et al., 1981; Chavkin et al., 1982). Its structure is H-Tyr-Gly-Gly-Phe-Leu-Arg-Arg-Ile-Arg-Pro-Lys-Leu-Lys-Trp-Asp-Asn-Gln-OH. Determination of the active conformation of dynorphin is an elusive and important goal for determining how the peptide interacts with the receptor to mediate its effects. Historically, structure−activity relationship studies have been used to focus on amino acid side chains required for activity. The lack of clear results from such studies have revealed that the active residues of dynorphin are still in question. For example, studies have indicated that the basic residues Arg^6, Arg^7, Lys^{11}, and Lys^{13} are key determinants for κ-selectivity (Turcotte et al., 1984; Snyder et al., 1992). However, the importance of Arg^6 and Arg^7 to selectivity could not be reproduced in a recent report (Kawasaki et al., 1993). Tyr^1 and Phe^4 of the N-terminal message sequence have long been thought to be required for dynorphin activity (Turcotte et al., 1984). A surprising report showed that a bulky aliphatic group could substitute, albeit weakly, for Tyr^1 (Gairin et al., 1988). Methods to examine the backbone conformations are even less definitive, as the outcome depends on the choice of solvent and conditions. Because dynorphin is linear, it samples a range of conformations in solution. Unless one can constrain the peptide or otherwise limit its conformational freedom, structural determination is difficult. Indeed, FTIR, NMR, and CD studies of dynorphin have shown that it is largely unstructured in solution (Renugopalakrishnan et al., 1988; Surewicz & Mantsch, 1989). In contrast, studies in this laboratory have shown dynorphin to be helical from about Gly^3 to Arg^9 in DPC micelles (Kallick, 1993).

There are several ways to reduce the inherent conformational flexibility in peptides that have been exploited [reviewed in Kessler and Steurnagel (1991)]. These include examining peptides in nonisotropic environments such as micelles and vesicles and cyclization of various peptide elements (i.e., introduction of disulfide bonds). Previous work in our laboratory and others has shown that DPC micelles have the ability to stabilize secondary structural elements in peptides (Kallick, 1993; Watts et al., 1995). DPC is well suited for NMR studies since the micelle-bound peptide can be studied in solution as opposed to solid state studies with artificial bilayers. In ideal cases, a complex forms which has motional characteristics of a macromolecule in the long correlation time regime (Henry & Sykes, 1994). DPC micelles can serve as a good model system for studying

† This work was supported by a grant from the Petroleum Research Fund, administered by the American Chemical Society. M.R.T. was supported in part by the Molecular Biophysics Training Program, NIH Grant 5T32 GM08277-07, and by the University of Minnesota Department of Medicinal Chemistry.

* To whom correspondence should be addressed.

⊗ Abstract published in *Advance ACS Abstracts,* January 15, 1997.

[1] Abbreviations: DPC, dodecylphosphocholine; dynorphin, dynorphin A (1−17); NMR, nuclear magnetic resonance; NOE, nuclear Overhauser effect; 1D and 2D, one and two dimensional; NOESY, nuclear Overhauser effect spectroscopy; TOCSY, total correlation spectroscopy; DIANA, distance geometry algorithm for NMR applications; TPPI, time-proportional phase incrementation; IRATR, infrared attenuated total reflectance; CSI, chemical shift index; RMSD, root mean square deviation; rMD, restrained molecular dynamics; SDS, sodium dodecyl sulfate; ppb/°C, parts per billion per degree Celsius; CD, circular dichroism; FTIR, Fourier transform infrared; TFE, 2,2,2-trifluoroethanol.

S0006-2960(96)01457-2 CCC: $14.00

the peptide/membrane interactions that may be important for receptor specificity (Henry & Sykes, 1994). In less than ideal cases, micelles present technical difficulties such as greatly increased line width and chemical exchange. Despite the difficulties, our approach to understanding peptide hormone activity has been to examine the conformations that are stabilized in the context of a model membrane, as it is believed that this more closely resembles the chemically anisotropic environment that a peptide hormone may encounter *in vivo*.

At least two ways in which a peptide hormone can interact with its receptor site may be envisioned. First, there is a direct interaction from the aqueous phase via a collision with solvent-exposed portions of the membrane-bound receptor. Second, there is the preadsorption of the peptide to the target cell membrane followed by subsequent interaction with the receptor. There is increasing evidence that peptide hormones encounter the lipid membrane before interacting with the receptor (Moroder et al., 1993; Schwyzer, 1995 and references within). The lipid membrane could serve numerous possible functions, including pooling the hormone at the membrane surface, changing the conformational search from a three-dimensional to a two-dimensional process, and locking the peptide into its bioactive conformation (Kaiser & Kezdy, 1987).

Dynorphin A (1−13) (henceforth called the 13mer) was first shown to bind to lipids by inserting its N-terminus into the hydrophobic phase of anionic liposomes (Gysin & Schwyzer, 1983). Infrared attenuated total reflection (IRATR) spectroscopy experiments subsequently showed that the 13mer formed an α-helix six to nine residues in length when bound to neutral lecithin membranes (Erne et al., 1985). It was also proposed at that time that the orientation of the α-helical region was perpendicular to the lecithin membranes. It was then proposed that the κ-selectivity of the 13mer and 17mer (dynorphin 1−17) is a consequence of the formation of an α-helix from residues Tyr^1 through Arg^9 upon insertion of the N-terminal "message" portion into the hydrophobic phase of the cell membrane (Schwyzer, 1986). The basis for the proposal is that κ-selectivity increases with the increasing amphiphilic moment of dynorphin analogs (Schwyzer, 1995 and references within). However, amphiphilic sequences may also form β-strands. The potential for dynorphin to form a β-strand was tested by an interesting analog study, in which the amphipathicity of a potential β-strand from residues 7 to 15 of dynorphin was retained while the sequence itself was changed (Vaughn & Taylor, 1989). Subsequent studies on the 13mer in methanol suggested the possibility of an extended or β-strand region between residues Arg^7 through Arg^9 (Lancaster et al., 1991). A more recent transferred-NOE study showed, however, some evidence for an α-helical region in the five N-terminal residues of the 13mer when bound to unilamellar vesicles (van Gorkum et al., 1992). Recent structure−activity studies on analogs of the 13mer constrained at the N-terminus in an arrangement thought to favor α-helix formation found that the analogs were slightly more κ-selective than the native 13mer (Arttamangkul et al., 1995). A previous report from our laboratory was the first to show that dynorphin is in an α-helical arrangement from residues Gly^3 through Arg^9 when bound to dodecylphosphocholine (DPC) micelles (Kallick, 1993). We now report a detailed study of dynorphin bound to DPC micelles using NMR spectroscopy, distance geometry in dihedral angle space, and restrained molecular dynamics and show that the peptide forms a well-defined α-helix from Phe^4 to about Pro^{10} and a less well-defined β-turn from residues Trp^{14} to Gln^{17}.

MATERIALS AND METHODS

Sample Preparation. Dynorphin A (1−17) (dynorphin) was obtained from Star Biochemicals (Torrance, CA), dodecylphosphocholine-d_{38} (DPC) from MSD Isotopes (Montreal), 99.9% D_2O from Cambridge Isotope Labs (Andover, MA), 99.9% D_2O with 0.75% 2,2,3,3-tetradeuterio-3-(trimethylsilyl)propionic acid (TSP) from MSD Isotopes, and sodium phosphate from Baker Analytical Reagents (Philipsburg, NJ). Most dynorphin/DPC spectra contained 4.88 mM dynorphin, 400 mM DPC-d_{38}, and 10 mM PO_4^{3-} at pH 3.4 in 90% H_2O/10% D_2O with an internal TSP standard for chemical shift referencing unless otherwise noted.

NMR Experiments. All NMR data were collected on either a Bruker AMX-500 or AMX-600 spectrometer and analyzed on a Silicon Graphics Personal Iris using FELIX v2.30 (Biosym, San Diego). The exchange experiment was performed by dissolving the peptide/DPC complex in H_2O and vacuum centrifuging to dryness. This was repeated several times. The peptide/DPC sample was then dissolved in D_2O, and NMR spectra were obtained after 24 h and after 1 week. The dynorphin ^1H resonances were assigned with information from total correlation spectroscopy (TOCSY) and nuclear Overhauser spectroscopy (NOESY) experiments as described below. The H_2O resonance was suppressed either by presaturation of the solvent peak during the relaxation delay (and the mixing time in the NOESY spectra) or by the use of a 3−9−19 pulse and tailored gradients (Piotto et al., 1992; Sklenar et al., 1993). TOCSY and NOESY spectra were collected at both 288 and 310 K to alleviate different spectral overlap problems at each temperature.

TOCSY experiments were obtained at 600 MHz with a spectral width of 7812.500 Hz in both dimensions using TPPI phase cycling (Marion & Wüthrich, 1983) with mixing times of 50 and 67 ms. Usually, 512 t_1 increments were acquired with 64 scans of 2048 complex points per t_1 value and 16 dummy scans prior to data acquisition to equilibrate the sample. The data were normally apodized in the t_2 dimension with a squared sine bell function (512 points, 90° phase) and in the t_1 dimension by application of a squared sine bell function (512 points, 90° phase) and then zero filled to yield a 2K by 2K real matrix.

Experiments with the standard NOESY pulse sequence (Macura & Ernst, 1980) for proton assignment, and the determination of distance restraints, were obtained at 500 MHz with a spectral width of 6578.947 Hz in both dimensions with TPPI phase cycling (Marion & Wüthrich, 1983). Experiments generally consisted of 440 t_1 increments with 64 scans of 2048 complex points per t_1 value. Apodization in the t_2 dimension was with a skewed sine bell squared function (440 points, 90° phase, and 0.9 skew) and in the t_1 dimension by linear prediction of one-third more points (Olejniczak & Eaton, 1990) before the application of a skewed sine bell squared function (590 points, 90° phase, and 0.9 skew) and zero filled to yield a 2K by 2K real matrix. A polynomial function in both dimensions was used for baseline correction of all NOESYs prior to measurement of

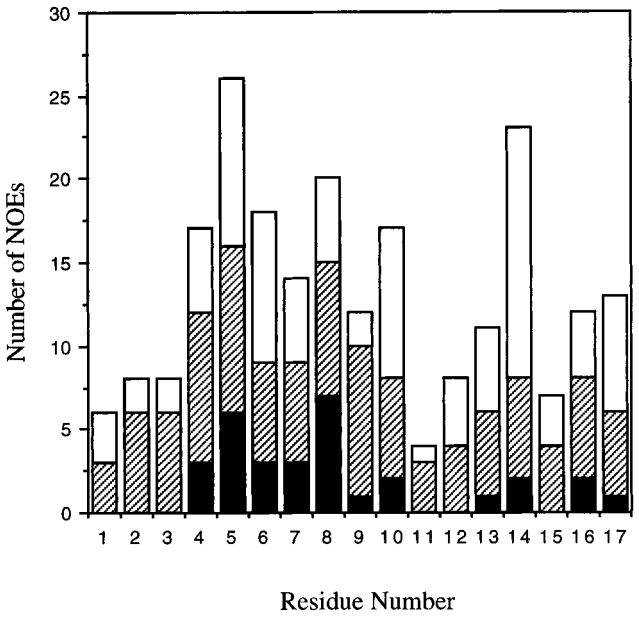

FIGURE 1: Number of NOEs versus residue number for dynorphin A (1−17) bound to DPC micelles; all interresidue NOEs are counted twice. Intraresidue NOEs are represented by open bars, sequential NOEs by cross-hatched bars, and NOEs between residues separated by two or more residues by solid bars.

cross peak volumes. Complete spectral assignments were made using the standard sequential assignment method (Wüthrich, 1986).

NOE Distance Restraint Calculations. Ranges of interproton distances were calculated by comparing the volume of the peak of three different "rulers": the Phe[4] 2,6H → 3,5H peak at 2.41 Å, the Trp[14] 1H → 7H peak at 2.82 Å, and the Asp[15] $\beta' \rightarrow \beta''$ peak at 1.78 Å (Kessler & Steurnagel, 1991). The volume of an individual peak was measured by integrating the 1D vectors representing a row and a column at a specific point and then dividing the product of these by the amplitude at that point (Holak et al., 1987). Each volume was normalized on the basis of the number of protons contributing to the peak. This method works well for peaks that are not clearly resolved since the point chosen need not be at the maximum, and curve fitting programs are available for calculating the 1D integrals of overlapped peaks (Roberts, 1993). The cross peaks were categorized into three classifications, 1.8−2.8 Å (strong), 1.8−3.3 Å (medium), and 1.8−5.0 Å (weak), for the distance geometry calculations described below. The NOEs are summarized in Figure 1.

Additional Restraints Derived from NMR Experiments. NOE information was supplemented with data on low amide temperature coefficients (Kallick, 1993) and slow exchange behavior. After the protonated peptide sample bound to DPC micelles was dissolved in D_2O, the amide peaks of Arg[6], Arg[7], Ile[8], Arg[9], and Trp[14] were still observable after 24 h. Restraints amounting to hydrogen bonds were added from the carbonyl oxygens of Gly[3], Phe[4], and Leu[5] to the amide protons of Arg[7], Ile[8], and Arg[9], respectively. Hydrogen bond restraints were only added after the initial DIANA calculations. No other hydrogen bond restraints were added, as no spectral evidence existed for helicity at the other residues. The H−O distance was defined as a range between 1.8 and 2.0 Å and the N−O distance between 2.7 and 3.0 Å in order to keep the hydrogen bond approximately linear (Williamson et al., 1985).

Structural Determination and Computational Modeling. The first step in the structural determination of dynorphin was the generation of 50 starting structures from random initial configurations with the DIANA algorithm (Güntert et al., 1991; Güntert, 1993). The initial input for DIANA calculations consisted of 184 distance restraints obtained from the NOESY experiments outlined above, as well as the hydrogen bond information described earlier. Pseudoatom modifications to the input data were made when necessary due to the lack of stereospecific assignments for the peptide's diastereomeric protons and the degeneracy of the 2,6 and 3,5 aromatic protons of tyrosine and phenylalanine (Wüthrich, 1986). Only short-range restraints are considered initially in DIANA calculations, with long-range restraints added to the variable target function as the strength of the van der Waals terms is increased (Güntert et al., 1991). Several rounds of DIANA calculations were performed with 50 structures generated each time. The output data were analyzed after each round of calculations for consistent violations of distance restraints. Corrected distance restraints were used in subsequent DIANA calculations. This cycle was repeated until the DIANA target functions obtained were very low, indicating that the resulting structures agree with the holonomic and experimental constraints. After the final DIANA calculation, no significant differences were seen between the α-helical region from residues Gly[3] through Pro[10] in all 50 structures generated. All of the final DIANA-generated structures also contained a β-turn from residues Trp[14] through Gln[17].

Twenty structures with the lowest target function from the final round of 50 DIANA generated structures were further characterized using energy minimization and restrained molecular dynamics (rMD). The structures were first minimized using the Discover module of Insight II v.2.30 (Biosym, San Diego) utilizing the AMBER force field (Weiner et al., 1986). Minimization was performed with the method of steepest descents until the change in energy was less than 0.001 kcal/Å. For all minimizations, as well as for the restrained molecular dynamics shown below, water was implicitly simulated with a distance-dependent dielectric constant of the form $\epsilon = r$. An infinite cutoff distance was used for determination of the nonbonded interactions, and flat-well distance restraints of 10 kcal mol^{-1} Å^{-2} were utilized; H-bond force constants of 10 kcal mol^{-1}Å^{-2} were also used. After minimization, the 20 structures were then subjected to 100 ps of constant temperature (300 K) restrained dynamics with the Discover module of InsightII v.2.30 (Biosym, San Diego) utilizing the AMBER force field (Weiner et al., 1986). The structures were allowed to equilibrate over the first 40 ps of the rMD runs and then averaged over the final 60 ps for subsequent analysis. The final structures were visualized and analyzed for energy and dihedral angle variations with Insight II v.2.30 (Biosym, San Diego). The structural statistics are summarized in Table 1.

RESULTS

Formation of the Peptide−Lipid Complex. Figure 2 shows the downfield ^{1}H NMR spectra of dynorphin in (a) aqueous DPC, (b) methanol, and (c) water. The spectrum in water displays narrow lines, limited chemical shift dispersion, and NH−C_αH coupling constants of about 8 Hz. The spectrum in methanol also displays narrow lines and limited chemical

Table 1: Structural Statistics for the Final Family of 20 Dyn A Structures

parameter	DIANA[a]	DIANA + rEM[b]	DIANA + rMD[c]
target function (Å^2)[a]	0.67 ± 0.20		
upper limit violations[a]			
number >0.2 Å	2.25 ± 1.89		
sum of violations (Å)	2.96 ± 0.53		
maximum violation (Å)	0.30 ± 0.09		
lower limit violations[a]			
number > 0.2 Å	0.00 ± 0.00		
sum of violations (Å)	0.01 ± 0.02		
maximum violation (Å)	0.01 ± 0.01		
van der Waals violations[a]			
number	0.20 ± 0.41		
sum of violations (Å)	1.18 ± 0.40		
maximum violation (Å)	0.17 ± 0.06		
pairwise RMSDs ± SD (Å)			
backbone RMSD residues 3−10	0.64 ± 0.24	0.73 ± 0.21	0.61 ± 0.26
heavy atom RMSD residues 3−10	2.11 ± 0.56	2.17 ± 0.50	1.87 ± 0.48
backbone RMSD residues 14−17	0.99 ± 0.41	0.96 ± 0.36	0.95 ± 0.35
heavy atom RMSD residues 14−17	2.28 ± 0.72	2.21 ± 0.65	2.07 ± 0.81
E_{bond} (kcal/mol)	23.8 ± 0.1	12.8 ± 0.8	12.6 ± 0.5
E_{θ} (kcal/mol)	39.6 ± 0.1	45.4 ± 4.3	46.9 ± 3.7
E_{ϕ} (kcal/mol)	60.3 ± 4.0	33.1 ± 3.9	34.2 ± 4.7
$E_{out\ of\ plane}$ (kcal/mol)	15.5[e]	2.3 ± 0.5	2.4 ± 0.4
$E_{H\text{-}bond}$ (kcal/mol)	−1.5 ± 4.4	−7.3 ± 1.1	−8.7 ± 1.6
E_{vdw} (kcal/mol)	278.1 ± 90.9	−5.6 ± 5.5	−7.8 ± 3.4
$E_{repulsion}$ (kcal/mol)	744.5 ± 105.3	379.7 ± 11.7	392.4 ± 9.6
$E_{dispersion}$ (kcal/mol)	−466.4 ± 18.5	−385.3 ± 14.2	−400.2 ± 10.5
$E_{Coulomb}$ (kcal/mol)	68.2 ± 22.2	−101.2 ± 25.3	−160.8 ± 17.1
E_{total} (kcal/mol)	484.0 ± 98.7	−20.5 ± 22.4	−81.2 ± 12.4
E_{force}[d] (kcal/mol)	82.0 ± 20.6	21.6 ± 4.5	21.3 ± 3.4
$E_{total+force}$ (kcal/mol)	566.0 ± 107.9	1.1 ± 29.3	−59.9 ± 12.8

[a] Averages ± SD for the 20 DIANA-generated structures with the lowest target function scores. [b] Averages ± SD for the 20 DIANA-generated structures after restrained energy minimization (rEM). [c] Averages ± SD for the 20 structures analyzed by restrained molecular dynamics (rMD). Each rMD run was averaged from 40 to 100 ps and then subjected to rEM. [d] E_{force} represents the total value of forcing from distance and dihedral restraints. [e] Out of plane value automatically assigned by Discover algorithm for DIANA-generated structures.

shift dispersion, although several resonances shift upfield. The largest chemical shift change is for one of the glycines, which moves downfield to about 8.8 ppm from its position in water to about 8.5 ppm. The methanol spectra also display NH−C_αH coupling constants of about 8 Hz. Taken together, these are indications of a small, linear peptide sampling a range of conformations. In contrast, the peptide in aqueous DPC undergoes marked changes in chemical shift and line width that level off at appropriate levels of DPC (Kallick et al., 1995). The downfield region in Figure 2a shows that the peptide resonances in the presence of DPC shift and broaden significantly. The peptide ^{1}H NMR peaks alone in water display weak but negative NOESY peaks, but the peptide ^{1}H peaks in DPC display NOESY peaks that are large and negative. This observation, taken together with the chemical shift dispersion and line widths, suggests that a structured molecule is bound to the lipid micelle. Further evidence for this is provided in Figure 3. Figure 3 shows the results of a proton/deuterium exchange experiment, in which the peptide/lipid complex was completely exchanged from H_2O into D_2O. Figure 3b shows the result after 24 h; Figure 3a shows the result after 1 week. After 24 hours the amide proton peaks for Arg^6, Arg^7, Ile^8, Arg^9, and Trp^{14} are still clearly visible. Clearly, exchange from H_2O into D_2O is considerably slower than one would expect for a peptide free in solution. Indeed, we observed several low amide temperature coefficients, indicating solvent inaccessibility (Kallick, 1993). Furthermore, the peptide/lipid spectra do not change significantly over a 30° temperature range (data not shown), indicating a stable complex which is not greatly affected by thermal motion over a limited range of temperatures. These are characteristics which are consistent with the formation of a stable peptide/lipid complex which is in the macromolecular correlation time regime.

Dynorphin A Chemical Shifts. Preliminary results showing NOEs indicative of an α-helix from Gly^3 to Arg^9 were reported previously (Kallick, 1993). Complete assignment of all the ^{1}H chemical shifts of dynorphin at 310 K are shown in Table 2. Due to the near degeneracy of the 14, 15, and 16 C_αH resonances with the solvent resonance at 310 K, additional NOESY data were obtained at 288 K to complete the resonance assignments and determine distance restraints. Figure 4 contains a portion of a 600 MHz NOESY at 288 K using gradient suppression of the H_2O resonance. The NH−C_αH cross peaks for Trp^{14}, Asp^{15}, and Asn^{16} at 4.63, 4.60, and 4.63 ppm, respectively, are clearly visible under these conditions. These assignments were verified with TOCSY experiments according to established procedures. Although some cross peaks are missing in this particular expansion, the combination of the lower temperature and optimal H_2O suppression allowed for the assignment of all of the peptide backbone and most of the total peptide resonances, as shown in Table 2. No significant differences in chemical shift were observed between the spectra at 288 and 310 K (data not shown). The lipid to peptide ratio for the experiments employed was *ca.* 80:1; under these conditions most of the peptide is stably bound to the lipid (Kallick et al., 1995).

Deviation of the experimental chemical shift from the random coil chemical shift is used as a diagnostic indicator of secondary structural elements in peptides and proteins (Wishart & Sykes, 1994). Figure 5 shows a comparison between the deviation from random coil for the full-length

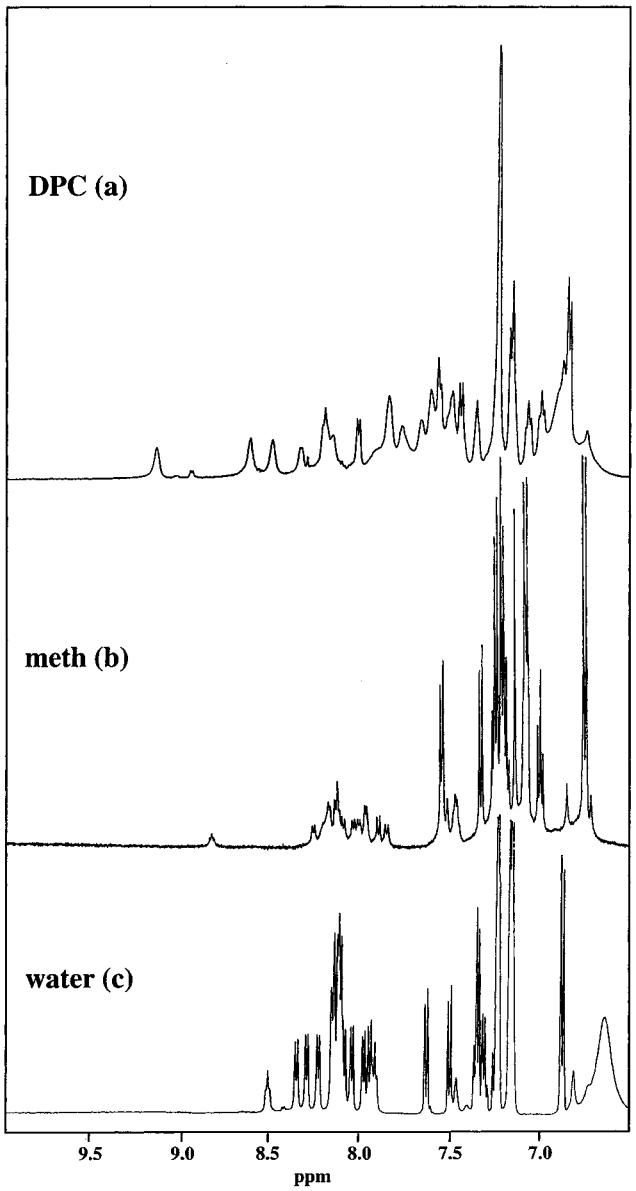

FIGURE 2: 500 MHz ^{1}H NMR spectra of dynorphin A (1−17) in (c) water, (b) methanol, and (a) dodecylphosphocholine (DPC) micelles. Spectra were obtained at 25 °C, *ca.* 4 mM peptide, and a lipid:peptide ratio of *ca.* 10:1 in (a).

dynorphin in aqueous DPC (solid bars) and the 13mer in methanol (open bars), as the chemical shifts are particularly informative when compared to the 13mer. The shifts are clearly indicative of a helix for dynorphin from both the $C_\alpha H$ shifts (Figure 5a) and the NH shifts (Figure 5b). It is interesting to note that, with only several exceptions, the shifts deviate from random coil values for the 13mer in the same direction but with less magnitude than the full-length dynorphin. The exceptions to this generalization are for Tyr^1, Pro^9, and Lys^{11} and Leu^{12} $C_\alpha H$ protons and the Gly^3 and Phe^4 amide protons. Lancaster, Epand and co-workers interpreted their data on the 13mer to be indicative of a partial β-strand from residues Arg^7 to Arg^9 (Lancaster et al., 1991). From comparison of the similarities in the chemical shift data, however, it is conceivable that the 13mer is at least partially helical. Since no evidence for a helix was observed in the 2D NMR data for the 13mer, it is likely that the peptide samples so many conformations that one family is not preferentially stabilized over another. In contrast, the full-length dynorphin is helical in one section (details *vide infra*)

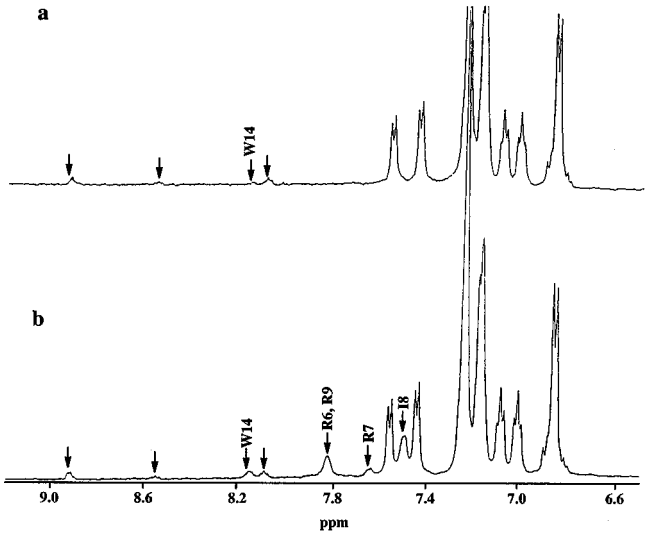

FIGURE 3: Proton exchange spectra obtained on dynorphin A (1−17) in DPC micelles at 500 MHz (a) 1 week after dissolving the peptide/lipid complex from H_2O to D_2O and (b) 24 h after dissolving the peptide/lipid complex from H_2O to D_2O. Note the long-lived amide protons after 24 h: Trp^{14}, Arg^6, Arg^9, Arg^7, and Ile^8. The unlabeled arrows indicate impurities in the lipid (Kallick et al., 1995).

as determined from Figure 5 and from the pattern of NOEs observed (Kallick, 1993).

A similar method of obtaining secondary structural information on peptides is the assignment of the chemical shift index (CSI) to the observed α-H proton shifts (Wishart & Sykes, 1994). A simple ternary scoring system is used for the chemical shifts of interest. An index score of −1 is given to any chemical shift more than 0.1 ppm lower than the estimated random coil value, and a +1 to any observed shift more than 0.1 ppm above the estimated random coil value. Any value falling within ±0.1 ppm of the random coil value is assigned a CSI score of 0. Any stretch of four consecutive −1 values determines an α-helical region in a peptide or protein. For the dynorphin/DPC complex there is a stretch of four consecutive −1 CSI values from residues Phe^4 through Arg^7 as shown in Figure 6. The last three residues of the peptide, Asp^{15}, Asn^{16}, and Gln^{17}, all have CSI scores of −1; however, the 2D NMR data coupled with the computational results (*vide infra*) show that the majority of the structures contain a type I β-turn at the C-terminus. From an analysis of the effects of β-turns on α-proton chemical shifts, a CSI of −1 would be expected at the $i + 1$ position of a type I β-turn (Ösapay & Case, 1994). In this example, Asp^{15} is at the $i + 1$ position of the turn. The $i + 2$ position of type I β-turns showed small variations from random coil in previous studies, so the CSI score of −1 for the Asn^{16} α-proton would not be predicted. However, the variation from random coil for the Asn^{16} α-proton is small (−0.11 ppm) and could be caused by a contribution from the type IV β-turn structures at the C-terminus as described below.

Structures of DPC-Bound Dynorphin. As previously reported, NOEs indicative of a helix were observed from residues Gly^3 through Arg^9 (Kallick, 1993). The NOEs are summarized in Figure 1, which indicates the number of NOEs per residue. Complete, unambiguous assignments (except for one aromatic proton; see Table 2) and the use of 184 NOEs permitted the generation of structures using

Table 2: ^{1}H Resonance Assignments for Micelle-Bound Dynorphin A (1−17) at 310 K

	chemical shift (ppm)			
residue	NH	αH	βH′, βH″	others
Tyr[1]		4.28	3.10, 3.10	2,6 H 7.15; 3,5 H 6.83
Gly[2]	9.11	3.94, 3.80		
Gly[3]	8.41	4.01, 3.84		
Phe[4]	8.59	4.33	3.25, 3.09	2,6 H 7.22; 3,5 H 7.14; 4H[a]
Leu[5]	8.11	3.87	1.75, 1.55	γH 1.45; $\delta H_3'$, $\delta H_3''$ 0.89, 0.81
Arg[6]	7.80	3.99	1.85,1.85	γH_2 1.66, 1.62; δH_2 3.18, 3.18; εNH 7.34
Arg[7]	7.62	4.16	1.88, 1.88	γH_2 1.68, 1.60; δH_2 3.17, 3.17; εNH 7.48
Ile[8]	7.46	4.10	1.81	γH_2 1.45, 1.19; γH_3 0.81; δH_3 0.81
Arg[9]	7.81	4.15	1.93, 1.93	γH_2 1.68, 1.68; δH_2 3.14, 3.14; εNH 7.34
Pro[10]		4.41	2.34, 2.34	γH_2 1.96, 1.79; δH_2 3.66, 3.48
Lys[11]	7.89	4.32	1.93, 1.77	γH_2 1.46, 1.46; δH_2 1.65, 1.65; ϵH_2 2.96, 2.96; ϵNH_3 7.74
Leu[12]	7.59	4.24	1.86, 1.68	γH 1.45; $\delta H_3'$, $\delta H_3''$ 0.82, 0.76
Lys[13]	7.71	4.31	1.77, 1.77	γH_2 1.30, 1.30; δH_2 1.64, 1.64; ϵH_2 2.96, 2.96; ϵNH_3 7.53
Trp[14]	8.14	4.63	3.28, 3.10	1H 10.49; 2H 7.22; 4H 7.55; 5H 7.00; 6H 7.06; 7H 7.45
Asp[15]	8.27	4.60	2.78, 2.61	
Asn[16]	8.19	4.63	2.79, 2.66	γNH_2 6.94, 7.64
Gln[17]	7.90	4.22	2.11, 1.91	γH_2 2.28, 2.28, δNH_2 7.60, 6.88

[a] Not observed.

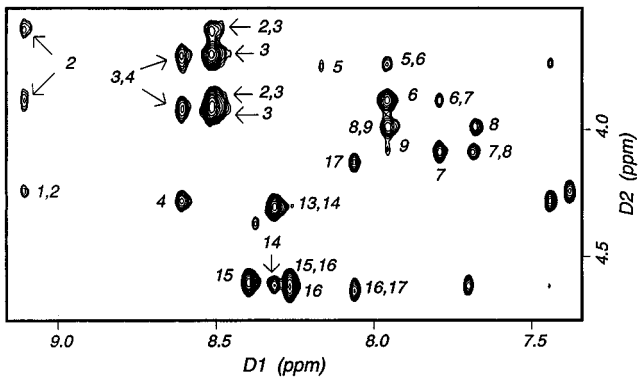

FIGURE 4: Expansion of a portion of the NH−C_αH fingerprint region of a 600 MHz gradient-enhanced NOESY spectrum (τ_m = 200 ms) of dynorphin in deuterated DPC micelles at 288 K. The sample is 4.88 mM dynorphin, 400 mM DPC, and 10 mM phosphate buffer in 90% H_2O/10% D_2O, pH 3.4. Suppression of the H_2O resonance was done with a 3−9−19 pulse and tailored gradients (Piotto et al., 1992; Sklenar et al., 1993). Helical NOEs were reported earlier (Kallick, 1993).

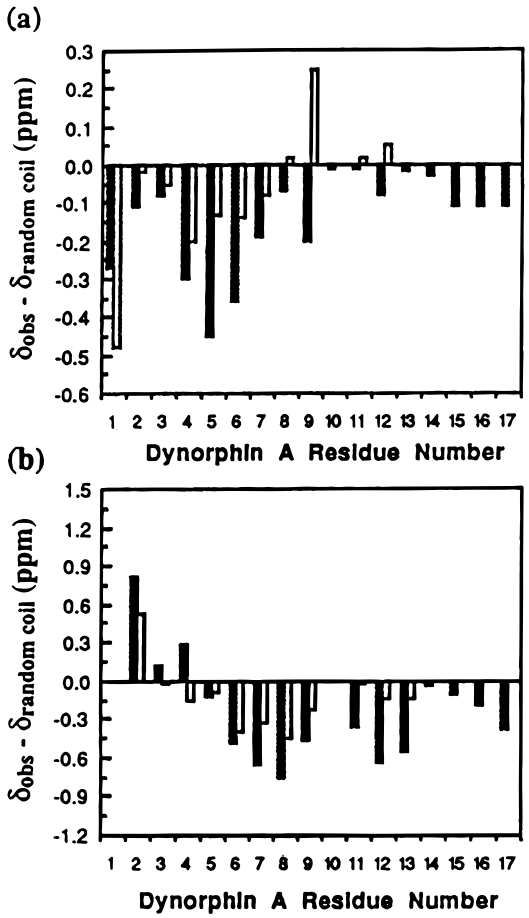

FIGURE 5: Comparison of variation from random coil ($\delta_{obs} - \delta_{random\ coil}$) between dynorphin A (1−17) (solid bars) and dynorphin A (1−13) (open bars) for (a) α-H shifts and (b) NH proton shifts. Data for dynorphin A (1−13) are from Lancaster et al. (1991) and random coil values are from Wishart and Sykes (1994).

distance geometry in dihedral angle space consistent with the experimental data. Subsequent restrained molecular dynamics simulations yielded final structures with low RMSDs and little variation in the helix region. Stereoviews of the 20 final structures superimposed over the backbone atoms of the well defined region (residues 3 through 10) are shown in Figure 7a. The variability in structure in the C-terminus and N-terminus appears to be a reflection of the lack of constraints in two regions. Specifically, the N-terminal residues, Tyr[1], Gly[2], and Gly[3], and the three residues on the C-terminal side of the α-helix, Lys[11], Leu[12], and Lys[13], have less NOEs than the other residues as shown in Figure 1. In contrast, many NOEs (≥13 per residue) are observed for the other residues. The variability in the final family of structures in the region of Lys[11], Leu[12], and Lys[13] is consistent with our observation that the Lys[13] amide was the only peak to have the same line width and similar chemical shift in water and in the aqueous lipid (at 7.71 ppm in Figure 2a). This implies that the Lys[13] amide proton is considerably exposed to water. In contrast, the Trp[14] was shown to be in a nonpolar environment by fluorescence emission spectroscopy (Tessmer & Kallick, 1997) and displays >15 NOEs to itself and to neighboring residues. This is important in the context of the discussion below, in which it is shown that the NMR data are consistent with a family of structures which all contain β-turns at the C-terminus.

Helical Region Analysis. Figure 7b contains the superimposition of the backbone atoms from residues Gly[3] to Pro[10] for the 20 dynorphin structures from the rMD calculations. Each structure represents an average of the final 60 ps of the corresponding rMD trajectory. The average backbone

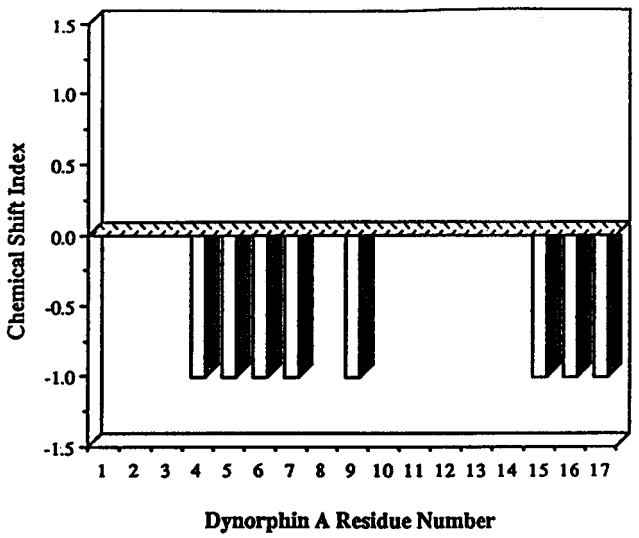

FIGURE 6: Chemical shift index plot for dynorphin A (1−17) at 310 K. A value of −1 represents a deviation from random coil ($\delta_{obs} - \delta_{random\ coil}$) of greater than −0.1 ppm. Random coil values are from Wishart and Sykes (1994).

RMSD from residues Gly[3] through Pro[10] of the 20 structures examined by rMD is 0.61 ± 0.26 and 1.87 ± 0.48 Å for the heavy atom RMSD, as shown in Table 1. As shown in Figure 7b, the peptide exists in an α-helical conformation from residues Gly[3] through Pro[10] when bound to DPC micelles. Examination of the individual structures with the amino acid side chains included reveals that, as expected, the helix is amphipathic, with the hydrophobic residues on one side of the helix and the hydrophilic residues on the opposite side of the helix. Five representative structures illustrating the amphiphathic characteristics of the well-defined helix are shown in Figure 8. The calculated average ϕ and ψ dihedral angles of residues Gly[3] through Lys[11] for the final 60 ps of the rMD trajectories are shown in Table 3. As can be seen from the data, the angles are close to the α-helical region ideal values of −57° and −47° for ϕ and ψ, respectively. In some residues there is a tendency for the ϕ value to be more negative than ideal and the ψ angle to be less negative than ideal. This is often observed in helical regions in proteins, as carbonyl oxygens of the helical residues are in a position which allows them to be hydrogen bonded to the corresponding amide proton in the helix as well as forming hydrogen bonds with the aqueous solvent (Creighton, 1993). Also, Arg[6] is in the middle of the helix, but its carbonyl oxygen is not able to hydrogen bond with the amide $i + 4$ residues away, as this is a proline residue and lacks an amide proton. This perhaps contributes to an opening up of the helix slightly, as indicated by the ϕ, ψ values for Arg[6] in Table 3. The Phe[4] carbonyl oxygen is less than 3 Å away from the Ile[8] amide nitrogen, forming a probable hydrogen bond. The Phe[4] carbonyl oxygen is also less than 3 Å away from the Arg[7] amide nitrogen as well, forming a potential bifurcated hydrogen bond with both Arg[7] and Ile[8].

In α-helices, the ideal hydrogen bond distance from the backbone carbonyl to the amide proton four residues away is 2.86 Å (Creighton, 1993). The data in Table 3 also show that the hydrogen bond distances for the Phe[4], Leu[5], and Arg[7] carbonyl oxygens to their corresponding amide nitrogens four residues away are 2.83 ± 0.11, 2.93 ± 0.06, and 2.87 ± 0.07 Å, respectively. From the dihedral angle data it is evident that the all-trans Pro[10] terminates the α-helix; however, the Lys[11] amide proton is still in a position to hydrogen bond with the Arg[7] carbonyl oxygen. The average distance from the Gly[3] carbonyl oxygen to the amide nitrogen of Arg[7] is 4.53 ± 0.61 Å. This distance is too long to be represented by a hydrogen bond and also shows higher variability than the other carbonyl oxygen to amide nitrogen distances in the α-helical region of the peptide. The early portion of the α-helix may not be as well defined as the latter part of the helix. There is a potential hydrogen bond between the Gly[3] carbonyl oxygen and the amide nitrogen of Arg[6], where the average carbonyl oxygen to amide nitrogen distance is 3.35 ± 0.66 Å.

C-Terminal Region Analysis. Fluorescence emission spectra indicate that Trp[14] is situated in a nonpolar environment (Tessmer & Kallick, 1997). Furthermore, an increased number of NOEs in the C-terminal region relative to the Lys[11], Leu[12], Lys[13] region are observed as shown in Figure 1. The final structures were analyzed in detail to determine if any trends emerged (Scanlon et al., 1995). Analysis of the dihedral angles from Trp[14] to Gln[17] revealed that the peptide adopts a β-turn from residues Trp[14] to Gln[17] in all final 20 structures. The absolute definition for a β-turn is that the $C_\alpha - C_\alpha$ distance from residues i to $i + 3$ of the turn be ≤7.0 Å (Ball et al., 1993). The average $C_{\alpha i} - C_{\alpha(i+3)}$ distance from Trp[14] to Gln[17] for the 20 dynorphin structures analyzed by rMD is 5.47 ± 0.64 Å, well within the turn definition. From an analysis of the average ϕ and ψ angles of the $i + 1$ and $i + 2$ residues for the last 60 ps of the rMD runs, two different types of β-turns can be identified. Twelve of the 20 structures form an ideal type I β-turn from residue Trp[14] to Gln[17], and the eight remaining structures fall into the classification of a type IV β-turn. Separation of the 20 final structures into the two different turn classifications yields Figure 7c for the type I β-turns and Figure 7d for the type IV β-turns. The average ϕ and ψ angles of the $i + 1$ residue (Asp[15]) for the type I β-turn structures are −57.4 ± 3.8° and −29.0 ± 6.1°, respectively, and for the $i + 2$ residue (Asn[16]) ϕ and ψ are −80.0 ± 10.0° and −3.3 ± 10.9°, respectively. These values correspond well with the ideal type I β-turn values of −60° and −30° for the $i + 1$ ϕ and ψ, respectively, and −90° and 0° for the $i + 2$ ϕ and ψ, respectively (Ball et al., 1993). The overall backbone RMSD for the 12 type I β-turn structures is 0.31 ± 0.09 Å from residues Trp[14] to Gln[17], clearly corresponding to a well-defined turn. The average distance from the Trp[14] carbonyl oxygen to the Gln[17] amide nitrogen in the type I β-turns is 3.06 ± 0.15 Å, indicating a possible hydrogen bond stabilizing the turn.

Examination of Figure 7d shows more variability in the type IV β-turns than the type I β-turns. The greater variability is reflected in the backbone RMSD of 0.93 ± 0.26 Å from Trp[14] to Gln[17]. The definition of a type IV β-turn is that two or more of the ϕ and ψ angles of residues $i + 1$ and $i + 2$ of the β-turn differ by more than 40° from the definitions of β-turn types I, I′, II, II′, III, and III′ (Ball et al., 1993). Each of the eight structures fits these criteria. Although there is some variability in the dihedral angles of individual structures, each structure fits the absolute requirement of a β-turn by having a $C_{\alpha i}$-$C_{\alpha(i+3)}$ distance of ≤7.0 Å. In the eight type IV β-turn structures, the average distance from the Trp[14] carbonyl oxygen to the Gln[17] amide nitrogen is 5.48 ± 0.98 Å, indicating the lack of a hydrogen bond.

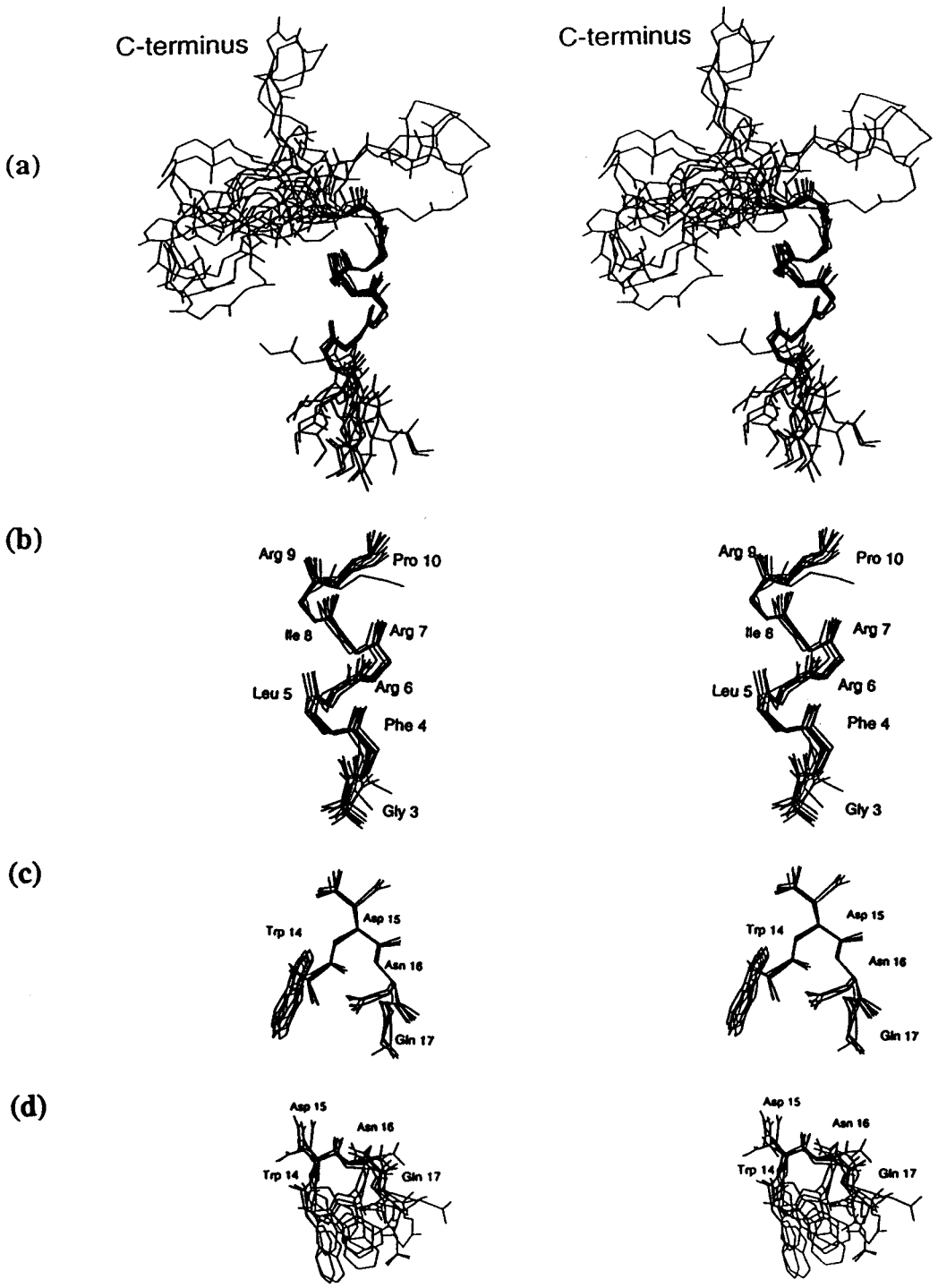

FIGURE 7: Stereoviews of the final structures of dynorphin A (1−17): (a) stereoview of the best fit of all backbone atoms for the 20 final dynorphin A (1−17) structures superimposed over the backbone heavy atoms from residues Gly[3] to Pro[10]; (b) stereoview of the helix region only, residues Gly[3] through Pro[10]; (c) stereoview of the C-terminal type I β-turns; (d) stereoview of the C-terminal type IV β-turns.

The lack of a hydrogen bond in the type IV β-turn structures is not surprising, based on a previous analysis of β-turns in the literature (Ball & Alewood, 1990).

Peptide Orientation with Respect to Micelle. Low amide temperature coefficients were observed previously for residues Leu[5] through Leu[12] and Trp[14] (Kallick, 1993). This, taken together with the amide proton exchange data, experimentally determined conformation, implied hydrogen bonds and fluorescence data (Tessmer & Kallick, 1997) are all consistent with a model of interaction in which the peptide is situated parallel to the surface of the micelle and embedded in the head region as schematized in Figure 9a. Other amphiphathic helices have been predicted to bind parallel to membrane surfaces (McDonnell et al., 1993) at the lipid−water interface. Dynorphin's apparent variability in conformation at the N-terminus (Figure 7a) suggests more exposure to water than would be likely if the peptide were inserted perpendicular into the micelle, as proposed early in dynorphin studies for anionic lipids (Gysin & Schwyzer, 1983). Either internal motion or the lack of experimental NOE constraints could account for the "fuzziness" at the N-terminus indicated by the overlay of the final 20 structures shown in Figure 7a. An important contributing factor in structure determination of a lipid-bound peptide is that some

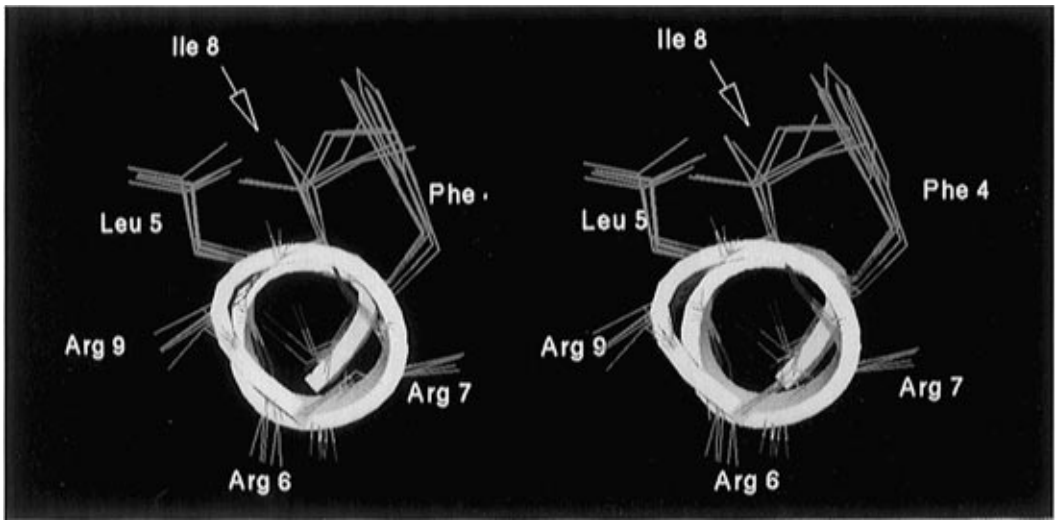

FIGURE 8: Stereoview of the helix viewed down the long axis with the hydrophobic residues (in blue) on the opposite side of the helix as the hydrophilic residues (in green). The side chains of all three arginines are truncated at the β-carbon for clarity.

Table 3: Average ϕ and ψ Dihedral Angles ± SD for the Last 60 ps of Constant Temperature Restrained Molecular Dynamics for the 20 Dynorphin Structures Examined and Distances ± SD for Key H-Bonds in the α-Helical Region of Dynorphin

residue	ϕ (deg)	ψ (deg)
Gly^3	-6.9 ± 80.4	-10.0 ± 52.1
Phe^4	-61.0 ± 17.3	-21.6 ± 13.3
Leu^5	-55.9 ± 3.3	-31.1 ± 2.9
Arg^6	-75.5 ± 4.9	-5.8 ± 9.4
Arg^7	-92.9 ± 5.7	-30.8 ± 6.6
Ile^8	-69.3 ± 5.4	-42.2 ± 12.2
Arg^9	-59.2 ± 7.2	-55.2 ± 8.8
Pro^{10}	-77.2 ± 12.4	-19.8 ± 28.7
Lys^{11}	102.7 ± 67.3	-1.9 ± 60.0
H-bonds		distance
Phe^4 O−Ile^8 N		2.83 ± 0.11
Leu^5 O−Arg^9 N		2.93 ± 0.06
Arg^7 O−Lys^{11} N		2.87 ± 0.07

interactions stabilizing the peptide/lipid complex are between peptide and *lipid*, requiring the determination of peptide/lipid NOEs. We cannot omit these types of interactions in this system and do indeed observe peptide/lipid NOEs in a different system (Watts and Kallick, in preparation, 1997). Theory indicates less mobility in the internal, aliphatic chains than the surface, head regions, suggesting that if the peptide were inserted perpendicular to the surface of the micelle with interaction in the internal region of the micelle, retarded amide exchange would be observed at the N-terminal residues. Instead, low amide temperature coefficients (Kallick, 1993), retarded amide exchange (Figure 2), and hydrogen bonds implied from the structural data suggest that residues Phe^4 through Lys^{11} and Trp^{14} have amide protons which are sequestered from solvent either by hydrogen bonds or by hydrophobic sequestering by the micelle. As the final structures indicate hydrogen bonds at three positions corresponding to $Phe^4CO \leftarrow Ile^8NH$, $Leu^5CO \leftarrow Arg^9NH$, and $Arg^7CO \leftarrow Lys^{11}NH$, the remaining amide protons, Phe^4, Arg^6, and Trp^{14}, are likely hydrophobically sequestered by the micelle. This is consistent with the model of interaction in which the hydrophobic face of the helix and the Trp^{14} is embedded in the head region of the micelle, shown schematically in Figure 9a. Each structure of the 20 final structures has the characteristic that the Trp^{14} side chain is on the same side of the peptide as the hydrophobic residues

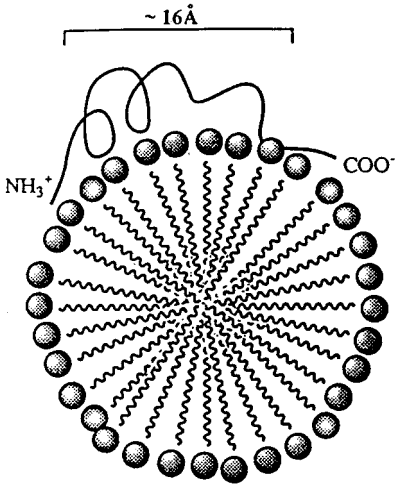

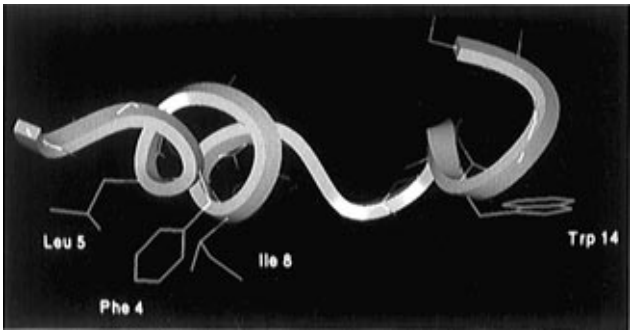

FIGURE 9: (a, top) Model of the interaction of dynorphin with the micelle. The average distance from Gly^3 to Trp^{14} (Cα to Cα) in the final, rMD-generated structures is 16 Å, indicated on the schematic. The average radius of the micelle at the concentrations employed is 23 Å (Kallick et al., 1995). (b, bottom) Representative structure of the 20 final structures showing the backbone atoms in pink and the hydrophobic residues in blue. The hydrophobic residues are proposed to anchor the peptide to the membrane such that the hydrophilic residues may interact with the receptor.

in the helix, further supporting the model of parallel interaction. One representative structure is shown in Figure 9b. The hydrophobic side chains noted in blue are all in a position to anchor the peptide to the micelle. Each residue highlighted has a large number of NOEs as shown in Figure 1, corresponding to a high degree of certainty in their location with respect to each other as well as in the overall structures.

DISCUSSION

Herein we have shown experimentally determined structural models of the full-length, endogenous ligand dynorphin in a model membrane. The structures determined here indicate that, in a micelle, dynorphin contains a well-determined α-helix from residues Phe^4 to about Pro^{10} or Lys^{11} and a β-turn from residues Trp^{14} to Gln^{17}, shown as one representative structure in Figure 9b. The structures are less well determined at the N-terminus and at the Lys^{11}, Leu^{12}, Lys^{13} region, the latter resulting in an apparent fuzziness at the C-terminus. Because of this, the type of β-turn cannot be unambiguously determined. Whether the variability in structure in these regions is due to internal motion or simply lack of constraints is not known. This is difficult to test without isotopic labeling.

The structures are significantly different from the conformation of the 13mer determined in methanol (Lancaster et al., 1991), although a comparison of the chemical shifts (Figure 5) suggests that the 13mer contains some helix. The natural breakdown pattern of prodynorphin to leucine-enkephalin is via dynorphin (1−8) and Dynorphin (1−17), the full endogenous ligand. Dynorphin (1−13) is found only as a minor product in *in vivo* isolates and is not the endogenous ligand for dynorphin's either opioid or nonopioid effects (Suda et al., 1983; Day et al., 1993). Even so, dynorphin (1−13) is commonly used in structure activity studies due to its similar potency and selectivity when compared to dynorphin (1−17). In a recent study, dynorphin (1-17) was shown to be more potent than dynorphin (1−13) in the inhibition of vasopressin release in the rat neural lobe via a probable κ-opioid receptor mediated pathway (van de Heijning et al., 1994). Since dynorphin (1−8) was not an inhibitor of vasopressin release in the rat neural lobe, it can be implied that the four C-terminal residues of dynorphin (1−17) do play a specific role in the higher potency in this case, and the increased potency of the 17mer is not simply due to resistance to proteolysis. Although the relationship of the structures presented here to the bioactive conformations is unknown, results presented here suggest the importance of an α-helix and perhaps a β-turn in mediating the peptide's actions.

Both the α-helix and the C-terminal β-turn may be a consequence of dynorphin's interaction with the micelle, or may be important structural features of the full-length peptide when bound to the cell membrane *in vivo*. The role of a C-terminal β-turn could conceivably be in increasing resistance to proteolytic degradation (Satoh et al., 1986; Young et al., 1987), conferring tissue-specific binding differences in κ-opioid receptors, or in mediating nonopioid effects of dynorphin. The α-helix could have multiple roles in positioning the amphipathic helix for interaction, as amphipathic helices have many roles at interfaces (Segrest et al., 1990). On the basis of the results presented here, it may be envisioned that the hydrophobic residues anchor the helix such that the hydrophilic residues may interact with the receptor. Indeed, the hydrophilic residues Arg^6, Arg^7, Lys^{11}, and Lys^{13} all appear to be important for dynorphin's activity *in vivo*. Although the importance of the last four residues of dynorphin has not been emphasized, these results suggest a critical role for Trp^{14} and the subsequent β-turn at the C-terminus. While the C-terminus may not be required for activity *in vitro*, it is possible that it plays a critical role in determining the "address" of dynorphin *in vivo*. Furthermore, the role of opioid peptides in nonopioid biological function has only recently become appreciated and is not very well understood.

There is much evidence in the literature to suggest that hormones interact with the cell membranes prior to diffusing to their receptor (Schwyzer, 1991; Moroder et al., 1993 and references therein), although this is difficult to prove with our current state of knowledge. More certain is the fact that structures may be determined in micelles, an environment which more closely resembles the chemically anisotropic environment of a peptide encountering a membrane-bound receptor *in vivo* than an organic solvent. The use of micelles is only now becoming more standardized and still presents considerable technical difficulties. For smaller polypeptides the advantage lies in reducing the number of conformational states the peptide may sample in solution, allowing structure determination in the macromolecular tumbling regime in the best of cases. Difficulties may arise for a number of reasons related to the properties of the peptide/lipid complex in solution. For example, there may be no long-range NOEs for an α-helix, whether the α-helix is membrane spanning or surface acting, as there are for α-helices flanking neighboring structural domains located in a protein. The atoms proximal to a peptide in a peptide/lipid complex are lipid atoms, which are normally perdeuterated so as to selectively visualize the peptide. As long-range NOEs are so difficult to come by, the resolution tends to be lower. Even if lipid/peptide NOEs are obtained, they are difficult to interpret, and the computational methods to incorporate the lipid−water interface in simulations are still in the early stages of development. Despite these shortcomings, studies of peptide hormones in model membranes can provide new insights on their three-dimensional structure and how the peptide interacts with model membranes.

ACKNOWLEDGMENT

The authors gratefully acknowledge Dr. Vikram Roongta of the Biochemistry NMR Center at the University of Minnesota, Mr. Paul M. Anderson of the University of Minnesota Supercomputer Institute, and Mr. Charles Watts from the University of Minnesota Department of Biochemistry for continued technical support.

REFERENCES

Arttamangkul, S., Murray, T. F., DeLander, G. E., & Aldrich, J. V. (1995) *J. Med. Chem. 38*, 2410−2417.

Ball, J. B., & Alewood, P. F. (1990) *J. Mol. Recognit. 3*, 55−64.

Ball, J. B., Hughes, R. A., Alewood, P. F., & Andrews, P. R. (1993) *Tetrahedron 49*, 3467−3478.

Brownstein, M. J. (1993) *Proc. Natl. Acad. Sci. U.S.A. 90*, 5391−5393.

Chavkin, C., James, I. F., & Goldstein, A. (1982) *Science 215*, 413−415.

Creighton, T. E. (1993) *Proteins: Structures and Molecular Properties*, W. H. Freeman, New York.

Day, R., Trujillo, K. A., & Akil, H. (1993) in *Handbook of Experimental Pharmacology* (Herz, A., Ed.) Vol. 104, pp 449−470, Springer-Verlag, New York.

Erne, D., Sargent, D. F., & Schwyzer, R. (1985) *Biochemistry 24*, 4261−4263.

Gairin, J. E., Mazarguil, H., Alvinerie, P., Botanch, C., J. Cros., & Meunier, J. C. (1988) *Br. J. Pharmacol. 95*, 1023−1030.

Goldstein, A. G., Fischli, W., Lowney, L. I., Hunkapiller, M., & Hood, L. (1981) *Proc. Natl. Acad. Sci. U.S.A. 78*, 7219−7223.

Güntert, P. (1993) *DIANA User's Manual and Instructions*, Version 2.1, Institut für Molekularbiologie und Biophysik Eidgenössiche Technische Hochschule-Hönggerberg, Zürich.
Güntert, P., Braun, W., & Wüthrich, K. (1991) *J. Mol. Biol. 217*, 517−530.
Gysin, B., & Schwyzer, R. (1983) *Arch. Biochem. Biophys. 225*, 467−474.
Henry, G. D., & Sykes, B. D. (1994) *Methods Enzymol. 239*, 515−535.
Holak, T. A., Scarsdale, J. N., & Prestegard, J. H. (1987) *J. Magn. Reson. 74*, 546−549.
Kaiser, E. T., & Kezdy, F. J. (1987) *Annu. Rev. Biophys. Biophys. Chem. 16*, 561−581.
Kallick, D. A. (1993) *J. Am. Chem. Soc. 115*, 9317−9318.
Kallick, D. A., Tessmer, M. R., Watts, C. R., & Li, C.-Y. (1995) *J. Magn. Reson., Ser. B 109*, 60−65.
Kawasaki, A. M., Knapp, R. J., Walton, A., Wire, W. S., Zalewska, T., Yamamura, H. I., Porrcea, F., Burks, T. F., & Hruby, V. J. (1993) *Int. J. Pept. Protein Res. 42*, 411−419.
Kessler, H., & Steurnagel, S. (1991) in *Peptide Pharmaceuticals* (Ward, D., Ed.) pp 18−46, Elsevier, New York.
Lancaster, C. R. D., Prasanna, K. M., Hughes, D. W., St.-Pierre, S. A., Bothner-By, A. A., & Epand, R. M. (1991) *Biochemistry 30*, 4715−4726.
Macura, S., & Ernst, R. R. (1980) *Mol. Phys. 41*, 95−117.
Marion, D., & Wüthrich, K. (1983) *Biochem. Biophys. Res. Commun. 113*, 967−974.
McDonnell, P. A., & Opella, S. J. (1993) *J. Magn. Reson., Ser. B 102*, 120−125.
Moroder, L., Romano, R., Guba, W., Mierke, D. F., Kessler, H., Delporte, C., Winand, J., & Christophe, J. (1993) *Biochemistry 32*, 13551−13559.
Olejniczak, E. T., & Eaton, H. L. (1990) *J. Magn. Reson. 87*, 628−632.
Ösapay, K., & Case, D. A. (1994) *J. Biomol. NMR 4*, 215−230.
Piotto, M., Saudek, V., & Sklenar, V. (1992) *J. Biomol. NMR 2*, 661−665.
Renugopalakrishnan, V., Rapaka, R. S., Huang, S. G., Moore, S., & Hutson, T. B. (1988) *Biochem. Biophys. Res. Commun. 151*, 1220−1225.
Roberts, G. C. K. (1993) *NMR of Macromolecules: A Practical Approach*, Oxford, New York.
Satoh, M., Yokosawa, H., & Ishii, S. (1986) *Biochem. Biophys. Res. Commun. 140*, 335−341.
Scanlon, M. J., Fairlie, D. P., Craik, D. J., Englebretsen, D. R., & West, M. L. (1995) *Biochemistry 34*, 8242−8249.
Schwyzer, R. (1986) *Biochemistry 25*, 6335−6350.
Schwyzer, R. (1992) *Chemtracts: Biochem. Mol. Biol. 3*, 347−379.
Schwyzer, R. (1995) *J. Mol. Recognit. 8*, 3−8.
Segrest, J. P., De Loof, H., Dohlman, J. G., Brouilette, C. G., & Anantharamaiah, G. M. (1990) *Proteins: Struct., Funct., Genet. 8*, 103−117.
Sklenar, V., Piotto, M., Leppik, R., & Saudek, V. (1993) *J. Magn. Reson., Ser. A 102*, 241−245.
Snyder, K. R., Stroy, S. C., Heidt, M. E., Murray, T. F., DeLander, G. E., & Aldrich, J. V. (1992) *J. Med. Chem. 35*, 4330−4333.
Suda, T., Tozawa, F., Tachibana, S., Demura, H., Shizume, K., Sasaki, A., Mouri, T., & Miura, Y. (1983) *Life Sci. 32*, 865−870.
Surewicz, W. K., & Mantsch, H. H. (1989) *J. Mol. Struct. 214*, 143−147.
Tessmer, M. R., & Kallick, D. A. (1997) Tryptophan 14 in Dynorphin A(1−17) is an Important Mediator of Peptide−Lipid Interaction, *Int. J. Pept. Protein Res.* (in press).
Turcotte, A., Lalonde, J. M., St. Pierre, S., & Lemaire, S. (1984) *Int. J. Pept. Protein Res. 23*, 361−367.
van de Heijning, B. J. M., Maigret, C., Koekkoek-van den Herik, I., Smelik, W. F. E., & van Wimersma Greidanus, Tj. B. (1994) *Neuropeptides 26*, 371−378.
van Gorkum, L. C. M., Lancaster, C. R. D., St. Pierre, S., Bothner-By, A. A., & Epand, R. M. (1992) in *Peptides, Chemistry and Biology: Proceedings of the 12th American Symposium* (Smith, J. A., & Rivier, J. E., Eds.) pp 233−234, Escom Science Publishers, Leiden.
Vaughn, J. B., Jr., Taylor, J. W. (1989) *Biochim. Biophys. Acta 999*, 135−146.
Watts, C. R., Tessmer, M. R., & Kallick, D. A. (1995) *Lett. Pept. Sci. 2*, 59−70.
Weiner, S. J., Kollman, P. A., Nguyen, D. T., & Case, D. A. (1986) *J. Comput. Chem. 7*, 230−252.
Williamson, M. P. (1990) *Bioploymers 29*, 1423−1432.
Williamson, M. P., Havel, T. F., & Wüthrich, K. (1985) *J. Mol. Biol. 182*, 268−315.
Wishart, D. S., & Sykes, B. D. (1991) *J. Mol. Biol. 222*, 311−333.
Wishart, D. S., & Sykes, B. D. (1994) *Methods Enzymol. 239*, 363−392.
Wüthrich, K. (1986) *NMR of Proteins and Nucleic Acids*, Wiley, New York.
Young, E. A., Walker, M., Houhgten, R., & Akil, H. (1987) *Peptides 8*, 701−707.

BI961457H